# Adsorption properties of α-type layered and pillared zirconium phosphite phosphonates with high specific surface area and porosities

## Supporting information

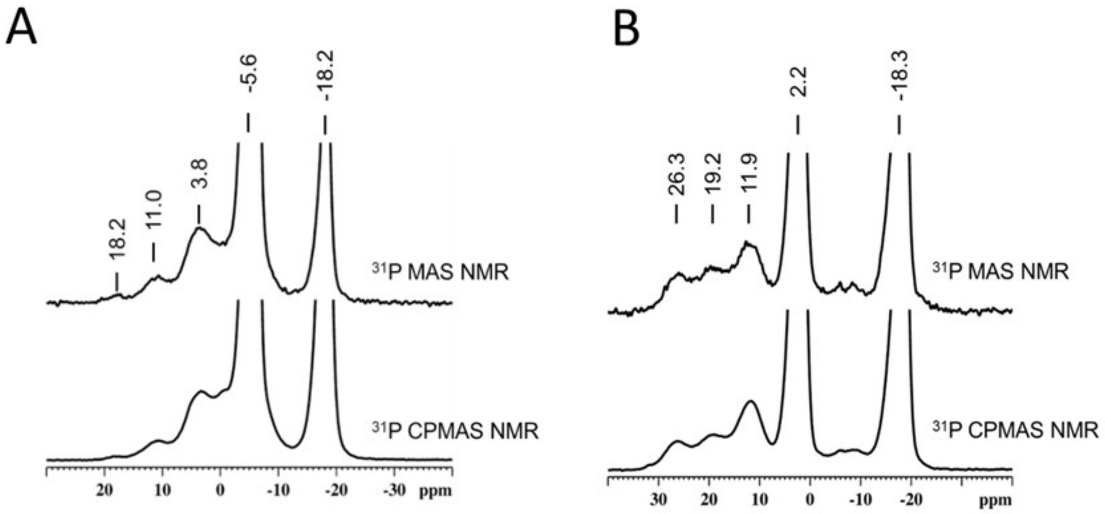

**Figure S1.** $^{31}$P MAS and CPMAS NMR spectra of: (A) Zr**P1**$_y$_1.5; (B) Zr**P2**$_y$_3.0.

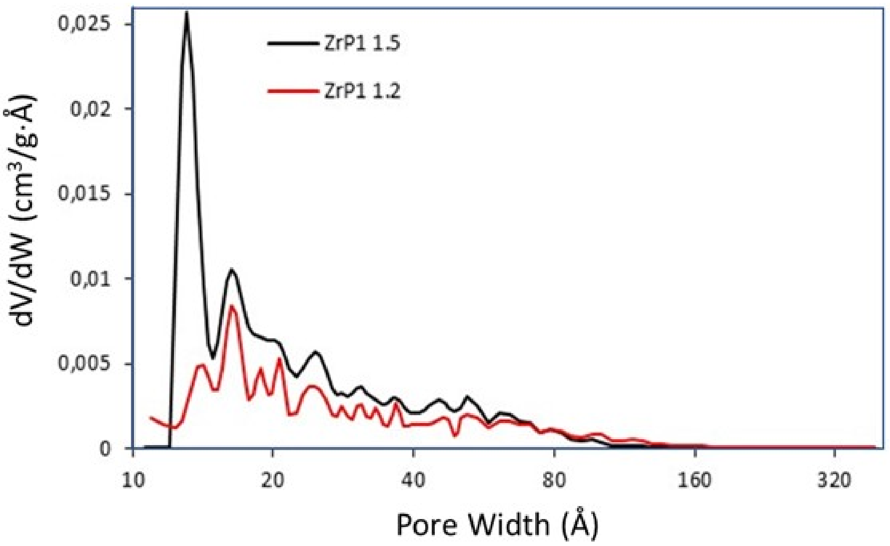

**Figure S2**. Pore size distributions of the Zr**P1$_y$**_R materials.

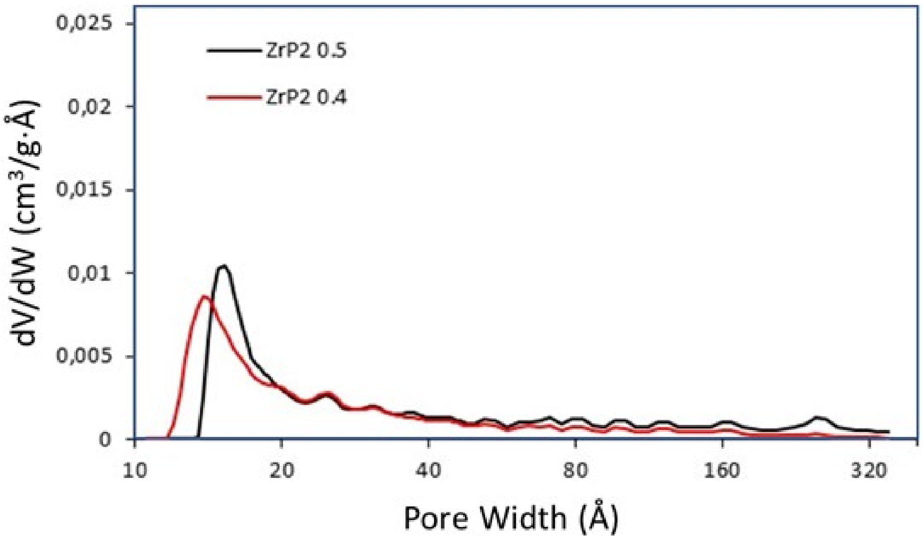

**Figure S3.** Pore size distributions of the Zr**P2**$_{\mathbf{y}}$_R materials.

| Absorbent | Main tipology of porosity | DCM uptake (mg/g) | T (°C) | SSA (m$^2$/g) Pore Volume (cm$^3$/g) | Ref. |
|---|---|---|---|---|---|
| HKUST-1 | micro | 1115 | 298 | 2327 0.81 | [1S] |
| UiO-66-5 | micro | 549.4 | 298 | 1447<br>0.61 | [2S] |
| n-MOF-5 | micro | 909 | 298 | 2982<br>1.86 | [3S] |
| n-MOF-5-NH$_2$ | micro | 1162 | 298 | 2346<br>1.22 | [3S] |
| ZIF-8/GO | micro | 240 | 298 | 861<br>0.32 | [4S] |
| NHPCS | micro/meso | 156 | 303 | 296<br>1.57 | [5S] |
| XAD-1600 | macro | 2292 (from solution) | 298 | 805 | [6S] |
| Activated carbon (ACJS) | macro | 159.6 | 298 | 1758<br>0.92 | [7S] |
| N/Al co-doped microporous carbon | micro | 611 | 298 | 1336<br>0.58 | [8S] |
| FAU and MFI zeolites | micro | 216.50 | 298 | 657<br>0.33 | [9S] |
| | | 179.14 | | 356<br>0.20 | |
| Porous carbons | micro | 416.89 | 298 | 944<br>0.38 | |
| N-doped porous carbons | micro | 426.70 | 298 | 1291<br>0.50 | [8S] |
| | | 576.64 | | 872<br>0.35 | |
| | | 611.29 | | 1336<br>0.58 | |

**Table S1.** DCM uptake and SSA of some porous absorbent materials

## Synthesis of PLA/ ZrP1$_{1.5}$_1.5 composite films

About 1 g of PLA powder was dissolved in 5 mL DCM at room temperature. About 2 g of Zr**P1**$_{1.5}$_1.5 gel in DCM (corresponding to 0.2 g of solid) were added to the PLA solution and the mixture was left under stirring for 24 hours. The mixture was then cast on a Petri dish and dried at 30 °C. The composite, containing 20 wt% of filler with respect to the polymer, will be indicated as PLA/ ZrP1$_{1.5}$_gel.

For comparison, a composite PLA/ Zr**P1**$_{1.5}$_1.5 was prepared by adding to the polymer solution 0.2 g of powder filler. The composite, containing 20 wt% of filler with respect to the polymer, will be indicated as PLA/ ZrP1$_{1.5}$_pwd.

## Preliminary Characterization of the PLA/ ZrP1$_{1.5}$ composite films

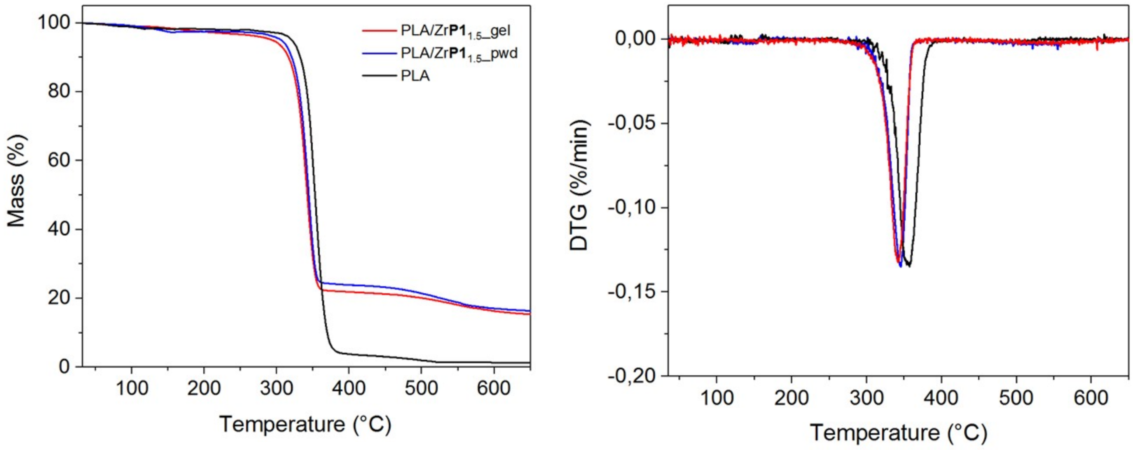

**Figure S4.** Thermogravimetric (left) and derivative thermogravimetric (right) curves of pure PLA (black line); PLA/ ZrP1$_{1.5}$_gel (red line); PLA/ ZrP1$_{1.5}$_pwd (blue line).

All samples exhibit similar thermogravimetric profiles, with a main mass loss between 300 and 400 °C. The filler shifts the polymer degradation to lower temperatures, as results from the peak position in the DTG curve; specifically, the temperature shift is 13 °C for PLA/ ZrP1$_{1.5}$_gel and 10 °C for PLA/ ZrP1$_{1.5}$_pwd.

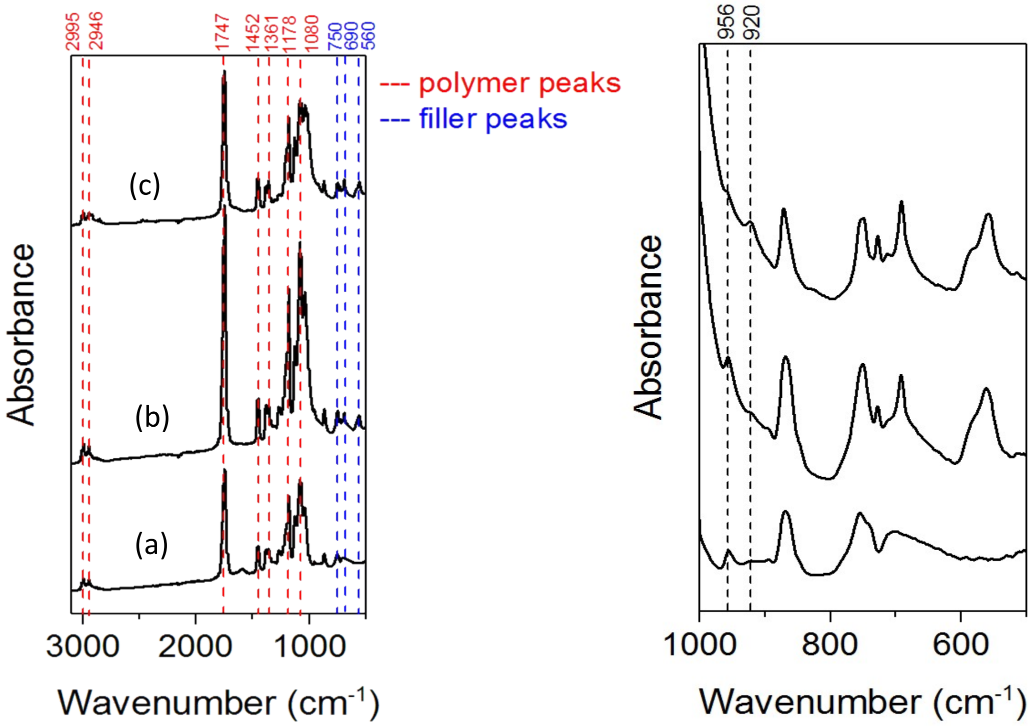

**Figure S5.** FTIR spectra of (a) pure PLA; (b) PLA/ ZrP1$_{1.5}$_pwd; (c) PLA/ ZrP1$_{1.5}$_gel, and their enlargement.

PLA shows characteristic stretching frequencies for C=O, –CH$_3$ asymmetric, –CH$_3$ symmetric, and C–O, at 1747, 2995, 2946 and 1080 cm$^{-1}$, respectively. Bending frequencies for –CH$_3$ asymmetric and –CH$_3$ symmetric are located at 1452 and 1361 cm$^{-1}$, respectively [10S]. The bands at 1178 cm$^{-1}$ and 1078 cm$^{-1}$ correspond to the stretching vibration modes of the C-O-C groups. The characteristic peaks of the filler at 560, 690, 750 cm$^{-1}$are observed. By enlarging the region at lower wavenumber, two bands, at 956 and 920 cm$^{-1}$ are observed, associate to the amorphous and crystalline phase, respectively [11S]; when passing from pure PLA to PLA/ ZrP1$_{1.5}$_gel, the disappearance of the band at 956 cm$^{-1}$ and the appearance of the band at 920 cm$^{-1}$ is observed, indicating an increasing crystallinity in the presence of the filler, especially if it is dispersed in the polymer matrix in the form of gel.

The above results suggest that the filler affects some polymer properties, in agreement with an interaction between the two components. Moreover, the filler effect is more pronounced when it is used in the form of gel in the same polymer solvent, probably due to its anti-aggregation action, promoting the polymer-filler interaction.

## References

1S. F. Tian, X. Zhang and Y. Chen, *RSC Adv.*, **2016**, *6*, 31214–31224.

2S. L. Zhou, X. Zhang and Y. Chen, *Mater. Lett.*, **2017**, *197*, 167–170.

3S. N. Missaoui, B. Gassoumi, S. Nasr, H. Kaur, A. Karayel, E. A. Lopez-Maldonado *et al.*, *J. Mol. Liq.*, **2025**, *418*, 126716.

4S. Y. Zhou, L. Zhou, X. Zhang and Y. Chen, *Microporous Mesoporous Mater.*, **2016**, *225*, 488–493.

5S. S. Liu, S. Wu, M. Li, Y. Li and X. Wang, *Ind. Crops Prod.*, **2024**, *209*, 118053.

6S. J. W. Lee, H. J. Jung, D. H. Kwak and P. G. Chung, *Water Res.*, **2005**, *39*, 617–629.

7S. S. H. Hsu, C. S. Huang, T. W. Chung and S. Gao, *J. Taiwan Inst. Chem. Eng.*, **2014**, *45*(5), 2526–2530.

8S. H. Zhang, Y. Zheng, Q. Ren, E. O. Fagbohun and Y. Cui, *Sep. Purif. Technol.*, **2025**, *360*, 130889.

9S. S. Kang, J. Ma, Q. Wu and H. Deng, *J. Chem. Eng. Data*, **2018**, *63*(6), 2211–2218.

10S. B. W. Chieng, N. A. Ibrahim, W. M. Z. W. Yunus and M. Z. Hussein, *Polymers*, **2014**, *6*, 93–104.

11S. N. Vasanthan and O. Ly, *Polym. Degrad. Stab.*, **2009**, *94*, 1364–1372.